



Abstract

Using small-angle neutron scattering we have imaged the magnetic flux-line lattice (FLL) in the *d*-wave heavy-fermion superconductor CeCoIn₅. At low field we observe a hexagonal FLL oriented along the crystalline [110]-direction. As the field is raised above 0.55 T the FLL undergoes a first-order reorientation and symmetry transition. Just above the transition the FLL is rhombic and gradually evolves towards square symmetry aligned along the [110]-direction as the field is raised to ~1 T. Measurements of the FLL reflectivity yields a constant form factor, independent of the applied magnetic field. This is in stark contrast to the exponential decrease usually observed as the field increases. The reason for this anomalous behavior is presently not clear, but we speculate that it is related to the magnetic properties of CeCoIn₅ and the close proximity to an antiferromagnetically ordered phase.

Introduction

CeCoIn₅ belongs to a new family of heavy-fermion superconductors, and with a $T_c = 2.3$ K it has the highest known critical temperature for heavy-fermion system¹. In addition CeCoIn₅ shows a plethora of fascinating electronic properties. Specific heat and thermal conductivity studies indicates a *d*-wave order parameter symmetry²⁻⁴, mediated by antiferromagnetic quantum fluctuations. Early measurements reported *d*_{xy} gap symmetry³, but recently there is an emerging consensus that superconductivity in CeCoIn₅ is of the *d*_{xy} type⁵. A possible explanation for this discrepancy is given in terms of a multi-band scenario with *d*_{xy} pairing on the heavy-electron sheets of the Fermi surface, and unpaired electrons on the light three-dimensional pockets⁶. Furthermore the close proximity of CeCoIn₅ to antiferromagnetic order leads to magnetic quantum critical point^{6,7}. Finally there have been reports of the observation of a Fulde-Ferrel-Larkin-Ovchinnikov superconducting state in CeCoIn₅⁸⁻¹⁰.

Fig. 1 shows an experimental phase diagram for CeCoIn₅. This shows the upper critical field becoming first order at low temperatures indicating Pauli limiting. For both field orientations the orbital limiting field, H_{orb} , is estimated to be ~12.5 T. The nature of the magnetic phase observed for $H \parallel c$ is still unknown. Although it has the same signature as the peak effect commonly observed close to H_{c2} , a softening of the FLL at this field and temperature seems unlikely.

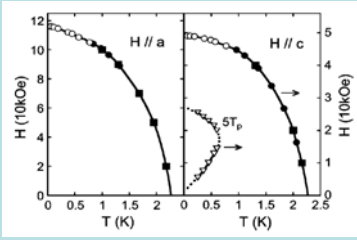


Fig. 1 Phase diagram for CeCoIn₅ obtained by magnetization measurements¹¹. The open circles indicates a first order superconducting transition. The triangles indicates the region where a hysteresis peak in the $M(H)$ loops are observed.

Previously we have reported on SANS measurements of the FLL in CeCoIn₅, where a hexagonal to square symmetry transition was observed¹².

Experimental Details

The small-angle neutron scattering (SANS) experiments were carried out at the D22 and D11 scattering diffractometers at the Institut Laue-Langevin, Grenoble, France. The single crystals of CeCoIn₅ used in the experiments were grown from excess indium flux, and had a $T_c = 2.3$ K and $B_{c2}(0) = 5.0$ T for fields applied parallel to the *c* axis. The sample was composed of three individually aligned single crystals with thickness 0.16 – 0.2 mm mounted side by side. The total mass of the sample was 86 mg. The rather thin samples were necessary, due to the strong absorption of low-energy neutrons by In. For all measurements, the sample was field cooled to 40 – 50 mK in a dilution refrigerator insert, placed in a horizontal field, superconducting cryomagnet. Magnetic fields in the range 0.4 to 2 T were applied parallel to the crystalline *c* axis and the incoming neutrons. Background subtraction was performed using measurements following a zero-field cooling.

References

1. C. Petrovic *et al.*, *J. Phys. Condens. Matter* **13**, L337-L342 (2001).
2. R. Movshovich *et al.*, *Phys. Rev. Lett.* **86**, 5152 (2001).
3. K. Izawa *et al.*, *Phys. Rev. Lett.* **87**, 057002 (2001).
4. H. Aoki *et al.*, *J. Phys. Condens. Matter* **16**, L13 (2004).
5. M. A. Tanatar *et al.*, *Phys. Rev. Lett.* **95**, 067002 (2005).
6. N. J. Curro *et al.*, *Phys. Rev. Lett.* **90**, 227202 (2003).
7. J. Paglione *et al.*, *Phys. Rev. Lett.* **91**, 246405 (2003).
8. T. P. Murphy *et al.*, *Phys. Rev. B* **65**, 100514 (2002).
9. H. A. Radovan *et al.*, *Nature* **425**, 51 (2003).
10. A. Bianchi *et al.*, *Phys. Lett.* **91**, 187004 (2003).
11. T. Tayama *et al.*, *Phys. Rev. B* **65**, 180504(R) (2002).
12. M. R. Eskildsen *et al.*, *Phys. Rev. Lett.* **90**, 187001 (2003).
13. D. K. Christen *et al.*, *Phys. Rev. B* **15**, 4506 (1977).
14. A. Yaouanc, P. Dalmas de Réotier, and E. H. Brandt, *Phys. Rev. B* **55**, 11107 (1997).
15. A. J. Berlinsky *et al.*, *Phys. Rev. Lett.* **75**, 2200 (1995).
16. J.-H. Xu, Y. Ren, and C. S. Ting, *Phys. Rev. B* **53**, R2991 (1996).
17. J. Shiraishi, M. Kohmoto, and K. Maki, *Phys. Rev. B* **59**, 4497 (1999).
18. M. Ichioka, A. Hasegawa, and K. Machida, *Phys. Rev. B* **59**, 8902 (1999).
19. M. R. Eskildsen *et al.*, *Phys. Rev. Lett.* **78**, 1968 (1997).
20. V. G. Kogan *et al.*, *Phys. Rev. B* **54**, 12386 (1996); *Phys. Rev. B* **55**, R8693 (1997); *Phys. Rev. Lett.* **79**, 741 (1997).
21. M. R. Eskildsen, Ph. D. thesis, Riso-R-1084 (1998).

Field Dependence of the Scattered Intensity

The FLL reflectivity is shown in Fig. 2 is determined by the magnetic field modulation around the vortices, and is proportional to the integrated scattered intensity of the Bragg peaks.

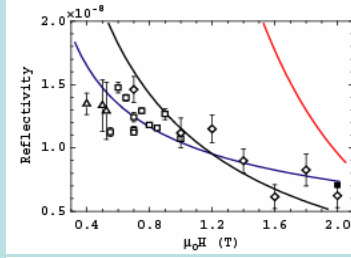


Fig. 2 FLL reflectivity. Curves described below.

Theoretically the FLL scattered intensity is determined by the reflectivity,

$$R = \frac{2\pi\gamma^2\lambda_n^2 t}{16\phi_0^2 q} |h(q)|^2 \quad q = 2\pi\sqrt{B/\phi_0}$$

where $\gamma = 1.91$ is the neutron gyromagnetic ratio, λ_n is the neutron wavelength, t is the sample thickness, ϕ_0 is the flux quantum, and q is the scattering vector¹³. The form factor, $h(q)$, for a square FLL is given by¹⁴:

$$h(q) = \frac{\phi_0}{(2\pi\lambda)^2} e^{-\pi B/B_{c2}}$$

Fig. 3 shows the form factor determined from the reflectivity in Fig. 3. The red curve in Figs. 2 and 3 is the theoretical prediction using $\lambda = 250$ nm from literature and the measured $H_{c2} = 5$ T. Substituting H_{c2} by the orbital critical field $H_{orb} = 12.5$ T and increasing λ to 430 nm yields the black curve. The best fit shown by the blue curve is obtained by a pure $1/q$ dependence corresponding to a vanishing core correction ($H_{c2} \rightarrow \infty$) and using $\lambda = 500$ nm.

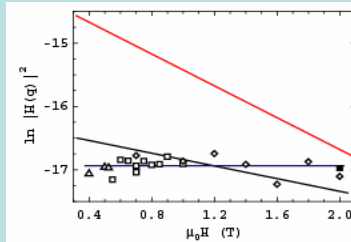


Fig. 3 FLL form factor. Curves described above.

Presently we do not have a detailed understanding of the FLL form factor in CeCoIn₅. Taken at face value a field independent form factor corresponds to an unphysical coherence length, $\xi = 0$. We speculate that this phenomena may be related to the magnetic properties of CeCoIn₅, as reflected in the field dependent diffuse background shown in Fig. 4.

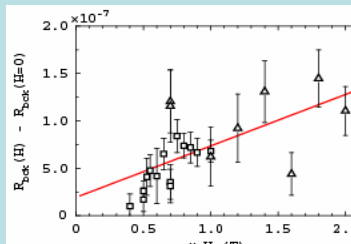


Fig. 4 Field dependence of diffuse background.

Acknowledgements

This work was supported by:



Flux-Line Lattice Symmetry Transition

Fig. 1 shows FLL diffraction patterns at three different values of the applied field. In Fig. 5 (a) the diffraction pattern shows 12 (2×6) Bragg peaks distributed evenly on a circle indicating two domains of a hexagonal FLL, aligned with along the crystalline [110]-direction.

As the field is increased above 0.55 T the FLL undergoes a transition to a rhombic symmetry, as seen in Fig. 5 (b). Again two domain orientations are observed, indicated by the 8 (2×4) Bragg peaks. At higher fields the FLL evolves towards a square symmetry, and the angular split between the Bragg peaks belonging to different domains is reduced as shown in Fig. 5 (c).

It should be pointed out that the rhombic distortion of the square FLL as the field is reduced would also lead to a hexagonal symmetry when the split becomes 30° . However, such a hexagonal FLL would be oriented along the crystalline [100]-direction, i.e. rotated 45° with respect to the FLL observed in Fig. 5 (a). This indicates that the transition at 0.55 T is a combined symmetry and orientation transition, and therefore most probably first order.

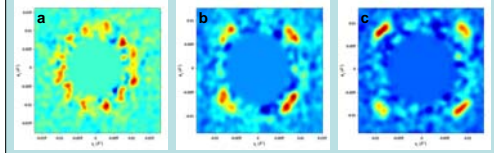


Fig. 5 FLL diffraction patterns for CeCoIn₅ with applied fields of 0.5 T (a), 0.55 T (b), and 0.75 T (c), after subtraction of background measurement. In addition the data are smoothed and the center of the image is masked off. The crystalline *a* axis is vertical.

The evolution of the transition, quantified by the FLL opening angle, is shown in Fig. 6. From this it is clear that the FLL have not reached a true square symmetry at 0.85 T which was the highest field where we could reliably fit and extract split angle. Measurements at 0.9 and 1 T still showed a split peak indicating a (weak) rhombic distortion.

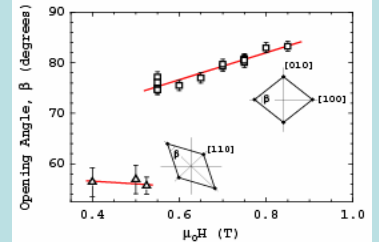


Fig. 6 FLL opening angle, β . The inserts show β for the low- and high-field orientation respectively.

There are at least two different mechanisms which can stabilize a square FLL. One is the gap anisotropy, which will favor a FLL orientation along the nodes of the superconducting gap¹⁵⁻¹⁸. However, even though the orientation of the gap nodes in CeCoIn₅ is still controversial, there is mounting evidence for a *d*_{xy} symmetry, inconsistent with the square FLL being stabilized by the gap anisotropy. The second, more likely driving mechanism responsible for driving the square FLL is a Fermi surface anisotropy, analogous to the situation observed in e.g. the borocarbide superconductors^{19,20}.

Déjà Vu? Form Factor in TmNi₂B₂C

Similar behavior have previously been observed in the nickel-borocarbide TmNi₂B₂C. In this material an antiferromagnetic state ($T_N = 1.5$ K) coexists with superconductivity ($T_c = 11$ K). Fig. 7. shows the form factor as a function of applied field, which remains constant up to 4 kOe.

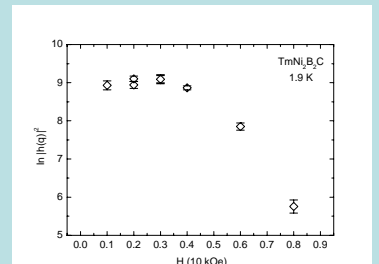


Fig. 7 Measured form factor for TmNi₂B₂C at 1.9 K²¹.